

Computerized-tomography (CT) analysis of 3D-printed porous bone ingrowth materials

Robert Kane, Joshua Auger, Brett English, Rakshak Nemiraj, Weidong Tong
Front End R&D, DePuy Synthes, Warsaw, IN.

Statement of Purpose: Sintered porous materials have a successful clinical history of allowing orthopedic implants to directly integrate with bone. Advances in additive manufacturing now allow for precise design of a porous material optimized for bone ingrowth. Previous methods of quantifying porosity and pore size have typically relied on 2D stereographic techniques (i.e. ASTM F1874) and only on planar surfaces, meaning these methods cannot be applied to more complex geometry (i.e. cylindrical surfaces) common on orthopedic implants. By utilizing CT methods both the interior and surface properties of porous materials can be non-destructively characterized for different geometries in three dimensions. The goal of this study is to first establish correlation between CT and gravimetric measures of porosity and then utilize this method to characterize porous structures produced by two different printer models.

Methods: Porous coating nominally 1.2 mm thick were applied onto a cylindrical geometry (6 mm dia.) as a coating or a fully porous monolith and utilizing laser powder bed fusion technology at three target porosities (Table 1). The second group includes flat coupons printed by two different printer models/manufacturers using identical design files (Table 2) All coupons were scanned using a Zeiss Metrotom 800 CT. Custom scripts in ImageJ and BoneJ were then used to obtain porosity and pore size. Gradients of both porosity and pore size were compiled, as well as a histogram of the pore diameter distribution. The monolith porosity in group 1 was calculated via a gravimetric method using calipers and balance.

Results: The porosities of the fully porous cylinders were measured gravimetrically, and all were within 4% of the as-designed porosity of 45, 55 or 65% (Table 1). The coating porosity, as measured by CT, was less than 2% different from the gravimetric measurement. With both the monolith and coating coupons using identical lattice designs, this correlation demonstrates that the CT method is accurately measuring the fraction of solid material with a porous lattice. The direct measurement of the cylindrical coating porosity was not previously possible through stereographic methods and is applicable to any arbitrary porous region.

Designed Porosity (%)	Fully Porous monolith(gravimetric) (n=5) (%)	Coating (CT) (n=3) (%)
45	41.7±0.8	41.5±1.5
55	55.9±0.3	54.2±0.1
65	68.3±0.5	69.2±0.7

Table 1. Porosity comparison between gravimetric porosity and CT-determined porosity on 5 mm cylindrical coupons.

For the comparison of coatings as produced by two different printer models both a bulk region (middle 80% of the coating thickness) and outer surface (top 0.38 mm of coating) were assessed. Pore size was measured using the BoneJ “Thickness” function, which uses an inscribed sphere approach to determine pore diameter. The porosity and mean pore diameters for each region of the coatings are listed in Table 2. While there are small differences between printers, there is a substantial uptick

in both pore diameter and porosity on the outer surface compared to the bulk measurement (Figure 1). While the pore size increase is due to the outer pores being open to the exterior, the porosity increase was not a feature of the design file and appears to be due to the printing process itself. In terms of function for bone ingrowth a higher outer porosity allows for more bone ingrowth while the somewhat less porous interior maintains mechanical strength. Note that the pore diameters here cannot be directly compared to the inferred 2D methods (i.e. line intercept methods).

Region	Printer 1		Printer 2	
	Porosity	Pore Dia. (µm)	Porosity	Pore Dia. (µm)
Bulk	62.9±1.3	416±8	60.5±0.9	401±4
Surface	72.6±0.4	578±6	73.1±0.6	607±44

Table 2. Porosity and mean pore diameter of coating lattice coupons produced on two different printers. (n=6 for Printer 1 and n=7 for Printer 2)

In addition to the mean values obtained for porosity and pore size, custom ImageJ scripts were written to measure porosity and pore diameter either slice-by-slice for flat coatings, or with radial ROIs for the cylindrical coupons to create gradient maps. An example coating gradient is pictured in Figure 1.

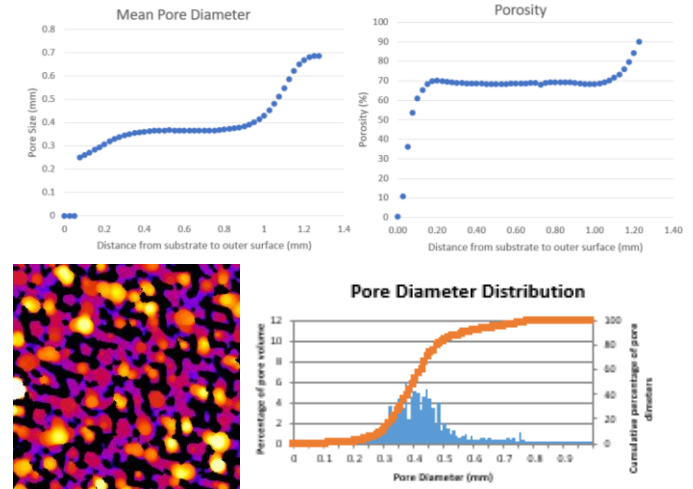


Figure 1. Mean pore diameter (top left) and porosity (top right) as a function of distance from substrate for a flat coating coupon. Bottom left is an example heat map of pore diameter (black is solid, color indicates larger pore size) from which a distribution can be obtained (bottom right).

Conclusions: CT methods developed for cancellous bone were successfully adapted to measure the porosity and pore structure of a 3D printed porous material. CT-based porosity was shown to correlate well to gravimetric porosity. The method was then used to assess both bulk and gradient measurements for coating coupons and can be adapted to any flat or cylindrical shape. Lastly, the ability to measure porosity gradients on 3D surfaces have demonstrated an increase in porosity closer to the surface of these 3D printed coatings.